Available online at www.sciencedirect.com

SCIENCE DIRECT

Developmental Biology 290 (2006) 177 – 188

DEVELOPMENTAL BIOLOGY

www.elsevier.com/locate/ydbio

VEGF-A signaling through Flk-1 is a critical facilitator of early embryonic lung epithelial to endothelial crosstalk and branching morphogenesis

Pierre-Marie Del Moral [a,b], Frédéric G. Sala [a], Denise Tefft [a,b], Wei Shi [a,b], Eli Keshet [c], Savério Bellusci [a], David Warburton [a,b,*]

[a] *Developmental Biology Program, Saban Research Institute, Children's Hospital Los Angeles, Department of Pediatric Surgery, USC Keck School of Medicine, 4650 Sunset Blvd., Los Angeles, CA 90027, USA*

[b] *Center for Craniofacial Molecular Biology, Keck School of Medicine and School of Dentistry, University of Southern California, CA, USA*

[c] *Department of Molecular Biology, The Hebrew University-Hadassah Medical School, Jerusalem, Israel*

Received for publication 20 November 2004, revised 10 October 2005, accepted 14 November 2005
Available online 22 December 2005

Abstract

Vascular endothelial growth factor-A (VEGF-A) signaling directs both vasculogenesis and angiogenesis. However, the role of VEGF-A ligand signaling in the regulation of epithelial–mesenchymal interactions during early mouse lung morphogenesis remains incompletely characterized. Fetal liver kinase-1 (Flk-1) is a VEGF cognate receptor (VEGF-R2) expressed in the embryonic lung mesenchyme. VEGF-A, expressed in the epithelium, is a high affinity ligand for Flk-1. We have used both gain and loss of function approaches to investigate the role of this VEGF-A signaling pathway during lung morphogenesis. Herein, we demonstrate that exogenous VEGF 164, one of the 3 isoforms generated by alternative splicing of the *Vegf-A* gene, stimulates mouse embryonic lung branching morphogenesis in culture and increases the index of proliferation in both epithelium and mesenchyme. In addition, it induces differential gene and protein expression among several key lung morphogenetic genes, including up-regulation of BMP-4 and *Sp-c* expression as well as an increase in *Flk-1*-positive mesenchymal cells. Conversely, embryonic lung culture with an antisense oligodeoxynucleotide (ODN) to the *Flk-1* receptor led to reduced epithelial branching, decreased epithelial and mesenchymal proliferation index as well as downregulating BMP-4 expression. These results demonstrate that the VEGF pathway is involved in driving epithelial to endothelial crosstalk in embryonic mouse lung morphogenesis.

Keywords: Vascular endothelial growth factor-A (VEGF-A); Fetal liver kinase-1 (Flk-1); Bone morphogenetic protein-4 (BMP-4); murine Sprouty-2 (mSpry-2); murine Sprouty-4 (mSpry-4)

Introduction

Embryonic lung development begins by evagination of the laryngo-tracheal groove from the foregut endoderm. Two distal buds subsequently branch laterally into the surrounding mesodermal mesenchyme. While extensive analysis of endodermal branching morphogenesis to form the lungs has been done (Chuang and McMahon, 2003; Hogan and Yingling, 1998; Warburton et al., 2000), relatively little is known about growth and differentiation of the lung mesenchyme. However, it is known that vasculogenesis, or in situ differentiation of endothelial precursors and assembly into a network, is already initiated within the mesenchyme as the lung evaginates from the foregut (Gebb and Shannon, 2000). Moreover, the Vascular Endothelial Growth factor (VEGF) family of ligands and their cognate receptors FMS-like tyrosine kinase 1 (Flt-1) or VEGF-R1, and Fetal Liver Kinase-1 (Flk-1) or VEGF-R2, affect a wide variety of physiological and pathological events (Ferrara et al., 2003).

VEGF-A is a specific endothelial cell mitogen (Leung et al., 1989), as well as playing a chemoattractant role for endothelial cells, osteoclasts and monocytes (Yoshida et al., 1996). In the mouse, alternative splicing of a single *Vegf-A* gene generates 3 isoforms: *Vegf* 120, 164, and 188, corresponding to the number of amino acids in each isoform (Shima et al., 1996). VEGF 164 is the major endothelial mitogenic factor among the 3 different VEGF isoforms (Keyt et al., 1996). While *Vegf-A* is restricted

* Corresponding author. Saban Research Institute, Children's Hospital Los Angeles, MS #35, 4650 Sunset Blvd., Los Angeles, CA 90027, USA. Fax: +1 323 671 3613.
E-mail address: dwarburton@chla.usc.edu (D. Warburton).

0012-1606/$ - see front matter © 2005 Elsevier Inc. All rights reserved.
doi:10.1016/j.ydbio.2005.11.022

to epithelial components (Miquerol et al., 1999) and both *Flt-1* (*Vegf-r1*) and *Flk-1* (*Vegf-r2*) are expressed by endothelial cells, Flk-1 appears to be the main receptor mediating the mitogenic and chemotactic effect of VEGF-A on the endothelium (Clauss et al., 1996). Flt-1, on the other hand appears to have a role in cell migration rather than cell proliferation (Barleon et al., 1996).

The essential role of the VEGF pathway during development has been demonstrated by gene targeting analysis. The loss of a single *Vegf-A* allele (*Vegf-A*$^{+/-}$) resulted in a lethal phenotype around mouse embryonic day 11.5 (E 11.5), associated with defects in the formation of the yolk sac vessels and of the dorsal aorta (Ferrara et al., 1996). A similar defect in embryonic blood vessel development was observed in heterozygous *Vegf-A* null embryos, and an even more severe defect has been observed in homozygous *Vegf-A* null embryos resulting in a lethal phenotype around mid-gestation (Carmeliet et al., 1996). Thus, the observed phenotypes suggest a dose-dependent effect of VEGF-A on embryonic vasculogenesis. Additionally, increased expression of VEGF-A has been shown to disrupt embryonic development, resulting in lethal heart defects around E14 (Miquerol et al., 2000).

Moreover, homozygous null *Flk-1* mutants die in utero at E8.5, lacking mature endothelial and haematopoietic cells, but also exhibiting an absence of blood island formation (Shalaby et al., 1995). Inactivation of the other VEGF receptor, Flt-1, also leads to a lethal phenotype around E 9.5. These embryos exhibit an excess of endothelial cells associated with a disorganized vascular network (Fong et al., 1995). However, the tyrosine kinase domain of *Flt-1* per se does not seem to participate in embryonic development, since no developmental abnormalities have been observed in embryos expressing a mutated *Flt-1* tyrosine kinase domain (Hiratsuka et al., 1998).

Taken together, the above data indicate a major role for VEGF-A and its cognate receptor Flk-1 during embryogenesis. During lung organogenesis, VEGF 120 and 164 isoforms are diffusely expressed in pulmonary epithelial and mesenchymal cells around E12.5, and are involved in controlling endothelial proliferation and the maintenance of vascular structure (Greenberg et al., 2002). Also, as epithelial morphogenesis progresses *Vegf-A* expression becomes restricted to the distal lung (Healy et al., 2000). This observation is postulated to be due in part to the relatively high affinity of VEGF-A for matrix components, that concentrates VEGF-A around the branching lung tips (Acosta et al., 2001; Ng et al., 2001).

To test the functional role of VEGF-A during early embryonic lung epithelial and vascular morphogenesis, we compared the effects of exogenous VEGF 164 with those of antisense ODN to *Flk-1* receptor on early embryonic lung morphogenesis in serumless chemically defined organ culture. Herein, we show that exogenous VEGF 164 increases embryonic lung epithelial as well as endothelial branching morphogenesis, whereas *Flk-1* antisense ODN decreases epithelial as well as endothelial lung branching in culture. VEGF-A signaling also differentially regulates the expression of BMP-4, *mSpry-2*, *mSpry-4* and *Sp-c* as well as the proliferation of both the epithelial and mesenchymal compartments. Therefore, we conclude that VEGF-A signaling plays a key functional role in mediating crosstalk between the epithelial, mesenchymal and endothelial compartments during epithelial and vascular branching morphogenesis of the early mouse embryonic lung.

Material and methods

Whole lung culture

Timed-pregnant Swiss webster mice were sacrificed on postcoitum day 11 (E11) or 12 (E12) and the embryos were removed. Lung primordia were isolated from embryos (E11 and E12) by microdissection. Dissection was carried out under sterile conditions using microophthalmic surgical instruments and a dissecting microscope. Early mouse embryonic lung lungs were cultures under serum-free, chemically defined conditions as reported previously (Jaskoll et al., 1988; Warburton et al., 1992). Embryonic lung explants were placed on 0.80-μm MF-Millipores filters (Millipore, Bedford, MA), supported by stainless-steel grids in Grobstein culture dishes (Flacon, Lincoln Park, NJ) and cultured in BGJb medium (Gibco, Grand Island, NY) supplemented with 0.1 mg/ml ascorbic acid and 50 units/ml penicillin/streptomycin. About 1 ml medium was added to each dish to establish an air fluid interface at the level of the explants. The cultures were maintained in 100% humidity with an atmosphere of 95% air and 5% CO_2 for 2 or 3 days. The medium was changed every day.

Exogenous VEGF and Flk-1 antisense ODN treatment

Exogenous recombinant murine VEGF 164 (R&D, Minneapolis, MN) was added to cultured E11 lung explants. A dose–response analysis was done using different VEGF 164 concentrations in the culture media (80 ng/ml, 100 ng/ml, and 150 ng/ml). There was an increased morphogenetic effect using 80 ng/ml and 100 ng/ml versus, but no additional differences were observed between 100 ng/ml and 150 mg/ml of VEGF 164. Therefore, a VEGF 164 concentration of 100 ng/ml was maintained during culture by replacing the media every 24 h. Phosphorothioate ODNs were purified by HPLC at the USC Comprehensive Cancer Center (Los Angeles, CA). The antisense oligomer sequence was selected following (Marchand et al., 2002) and had specific characteristics (no more than three consecutive guanosines, the incapacity to form hairpins without or minimal capacity to dimerize together, and was 18 bases in length). The murine *Flk-1* cDNA was obtained from GenBank (Accession Numbers X70842). Antisense or scrambled ODNs were added separately to the culture medium at a final concentration of 40 μM. The oligonucleotides used were separately: *Flk-1* antisense ODN 5′-AgT ATg TCT TTC TgT gTg-3′, versus scrambled ODN 5′-TTT CTg gTA TgC ATT gTg-3′ as negative control. The oligomers were used under sterile conditions.

Quantification of branching morphogenesis

We quantified branching on whole-mount lung explants by counting the number of epithelial sacs around the periphery of the lung explants. Transillumination was used to detect structures and photomicrography was used to record permanent images. Branching was counted for four to six lungs per data point and statistical significance was determined by ANOVA and *t* test (values were considered significant if $P < 0.05$).

Flk-1$^{nLac\text{-}Z/+}$ *and Bmp-4*$^{LacZ/+}$ *staining*

Heterozygous *Flk-1*$^{nLac\text{-}Z/+}$ and *Bmp-4*$^{LacZ/+}$ mice (Lawson et al., 1999; Shalaby et al., 1995) were, respectively, obtained from Jackson Laboratories and as a gift from Dr. Hogan. Dissected heterozygous lungs were fixed in 4% paraformaldehyde and reacted with X-gal as described by (Lawson et al., 1999). Vibratome sections (20 μm) of the caudal lobe were then made.

In vitro assay of isolated lung epithelium and mesenchyme

E12.5 mouse lung were isolated and treated with undiluted dispase (BD Biosciences, San Jose, CA) for 30 min at 4°C. The lung mesenchyme was separated from the epithelium using fine tungsten needles and transferred into Matrigel™, diluted 1:1 with culture medium (5% FCS (DMEM: F12) penicillin/streptomycin + glutamine) in a four well dish (Nalgene Nunc, Rochester, NY). Polymerization of the Matrigel™ was triggered at 37°C for 30 min. After polymerization, 500 μl of culture medium containing the growth factor VEGF (150 ng/ml) was gently added to the Matrigel™ layer. The respective epithelial versus mesenchymal explants were grown for 48 h at 37°C in a 5% CO_2 incubator. Explants were fixed in 4% paraformaldehyde and reacted with X-gal as described by (Lawson et al., 1999).

RNA extraction and reverse transcription

Lungs were harvested and total RNA was extracted using Total RNA Isolation kit (5′Prime–3′Prime, West Chester, PA). The RNA was reverse-transcribed by incubating the samples at 37°C for 1 h in 20 μl of 10 mM Tris (pH 8.4), 2 mM $MgCl_2$, 50 mM KCl, 1 mM dithiothreitol, 0.5 mM dNTP, 5 units ribonuclease inhibitor, 100 pmol oligo (dT)12–18 and 200 units MMLV reverse transcriptase (USB, Cleveland, OH). The reaction was terminated by incubation for 5 min at 95°C. Spectrophotometry was used to determine cDNA concentration (A_{260}, 50 μg/ml). The reverse-transcribed samples were then used for competitive PCR.

Competitive RT-PCR

Competitive RT-PCR was performed as previously described (Zhao et al., 1998) to determine the effects of treatment on mRNA levels in the lungs. The same primers were used to amplify both cDNA and competitor for each gene of interest. A cDNA/competitor scale was designed using a fixed concentration of competitor with scaled concentrations of cDNA. The log of cDNA/competitor was plotted against the target concentration, resulting in a coefficient $r^2 > 0.98$. Competitive PCR quantification provides an accurate assessment of mRNA levels and is reliable in the absence of contaminating DNA species. PCR was performed in a Robocyler (Stratagene, La Jolla, CA). The first cycle consisted of an initial 3 min denaturation at 94°C, annealing at 62°C for 1 min, and extension at 72°C for 2 min. The next 30 cycles were similar except for a 1-min denaturation period and in the last cycle the extension period lasted 5 min. The reaction mixture contained 20 pmol primers, 10 mM Tris (pH 9.4), 50 mM KCl, 2 mM $MgCl_2$, 0.01% gelatin, 0.1% Triton X-100, 100 μM dNTP and 0.5 units of Advantage Clontech DNA polymerase (Clontech, Palo Alto, CA). A known amount of competitor was added to products of reverse transcription. Competitive PCR, using *β-actin*, was also performed with all samples as a positive control. The primers used for amplification were as follows: *Fgf10* forward primer, 5′-CACATTGTGCCTCAGCCTTTCC-3′; *Fgf10* reverse primer, 5′-CC TGCCATTGTGCTGCCAGTTAA-3′ (predicted size 505 bp); *mSpry2* forward primer, 5′-TGTGAGGACTGTGGCAAGTGC-3′; *mSpry2* reverse primer, 5′-TTTAAGGCAACCCTTGCTGG-3′ (predicted size 300 bp); *Bmp4* forward primer, 5′-TCCATCACGAAGAACATC-3′; *Bmp4* reverse primer, 5′-TAGTCGTGTGATGAGGTG-3′ (predicted size 238 bp); *Shh* forward primer, 5′-GCTGCTGGCCAGATGTTTTCTG-3′; *Shh* reverse primer, 5′-TCCAGGCCACTGGTTCATCACA-3′ (predicted size 351 bp); *Flk-1* forward primer, 5′-ACTGGAGCCTACAAGTGCTCGT-3′; *Flk-1* reverse primer, 5′-TGAGGTTTGAAATCGACCCTCG (predicted size 181 bp); *Sp-c* forward primer, 5′-TGGTCCTTGAGATGAGCATCGG; *Sp-c* reverse primer, 5′-GTAGAGTGGTAGCTCTCCACAC (predicted size 360 bp); *mSpry4* forward primer, 5′-GTGTCTGGTGCAAGGTATCTTC; *mSpry4* reverse primer, 5′-TCAGAAAGGCTTGTCAGACCTG (predicted size 300 bp).

Quantification of cDNA and statistical analysis

Target cDNA and competitor PCR products were separated by electrophoresis in a 3% agarose gel (3:1 mixture of Nusieve and Seakem; FMC, Rockland, ME). The gel was run on a submarine gel apparatus (C.B.S. Scientific Co., Del Mar, CA) and stained with 5 μg/ml ethidium bromide. Photographs were taken with Polaroid 667 film and the intensity of the bands was determined by densitometry.

Western blot analysis

Cultured embryonic lungs were disrupted immediately in SDS buffer containing protease inhibitors and sodium fluoride. Equal amounts of total lung protein (50 μg) from each assayed sample were used for chemiluminescent Western analysis (Roche Molecular Biochemicals) on Immuno-Blot PVDF membrane (Bio Rad, Hercules, CA). Immunoblotting was performed using antibodies against human BMP-4 (R&D systems, Minneapolis, MN), and Mouse anti-actin (ICN Biomedicals, Aurora, OH) at recommended dilutions (1:1000 for the BMP-4 antibody, and 1:10,000 for the actin antibody).

Analysis of lung proliferation ex vivo

Dehydrated lungs were embedded in paraffin and sections (6 μm) were cut. Proliferation was measured using the PCNA kit (Zymed) following the manufacturer's instructions. All cells were counted and scored in five photomicrographs, at 50× magnification, of random portions of a section of treated versus control lungs. At that stage, it was possible to distinguish clearly between epithelial and mesenchymal cells and the PCNA index was calculated for the epithelial and mesenchymal compartments.

Data analysis

The data in the present study were expressed as mean ± SD, and the significance of variances between means was evaluated by ANOVA followed by Student's *t* test. *P* values less than 0.05 were considered to be statistically significant.

Results

VEGF does not induce branching of isolated lung endoderm but does induce amplification of Flk-1-positive cells in the mesenchyme

We initially analyzed the expression pattern of Flk-1 receptor in E14.5 *Flk-1*$^{nLacZ/+}$ lungs. The beta-galactosidase staining corresponding to *Flk-1* expression in this tissue revealed exclusive expression of the receptor in the mesenchyme (Figs. 1A, B). We then isolated E12.5 embryonic lung endoderm from mesenchyme and cultured it in matrigel for 48 h in the presence of VEGF 164. We observed that VEGF 164 did not induce epithelial branching in isolated lung endoderm (Figs. 1C, D). FGF10, used as a positive control in our experiments, induced growth and budding as already described (Bellusci et al., 1997), therefore attesting to the viability and responsiveness of the isolated endoderm (data not shown). In contrast, mesenchymal explants cultured with VEGF 164 exhibited striking increases in β-galactosidase staining representing *Flk-1*-positive cells (Fig. 1F). Control mesenchyme did not contain any *Flk-1*-positive cells (Fig. 1E).

VEGF 164 stimulates epithelial branching morphogenesis on the whole lung in culture

We initially observed that lung buds from 11-day mouse embryos cultured in vitro for 24 h, 48 h, and 72 h in a

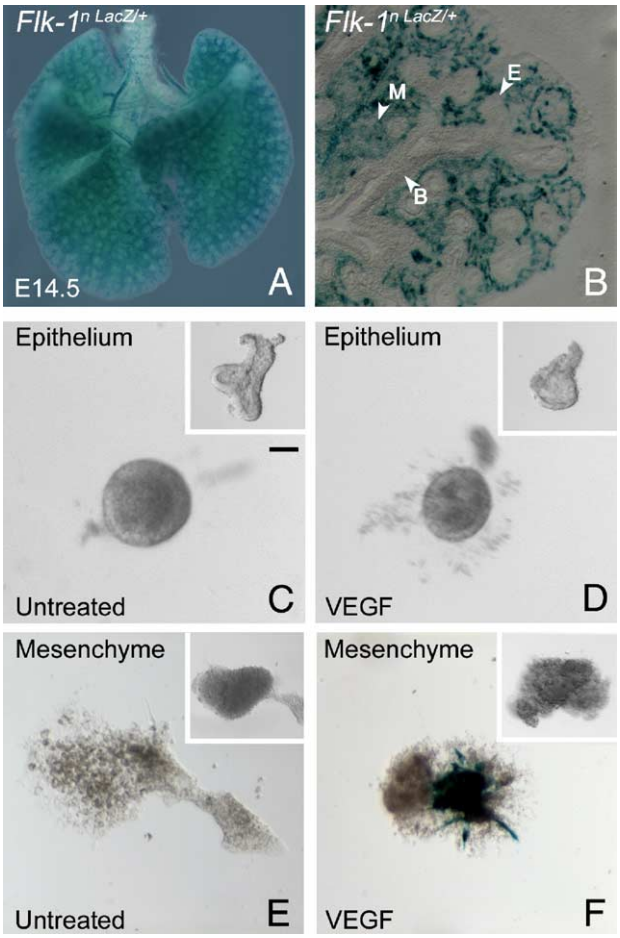

Fig. 1. VEGF 164 does not induce branching of isolated lung endoderm but does induce differentiation of *Flk*-1-positive cells in isolated mesenchyme. Analysis of the expression pattern of *Flk-1* on E14.5 *Flk-1*$^{n\ LacZ/+}$ lungs on whole lung (A) and 30 μm vibratome section of the caudal lobe (B) show the staining corresponding to *Flk-1* expression only in the mesenchyme (arrowhead M) and not in the bronchial and distal endoderm (arrowhead B and E, respectively) at that stage of development. Culture of isolated embryonic lung endoderm (C, D) versus mesenchyme (E, F) in matrigel from 0 h (insets in C–F) to 48 h (C–F) in presence or absence of VEGF 164 revealed an exclusive morphogenic effect on the mesenchyme (F). β-galactosidase staining representing *Flk-1*-positive cells is detected only in VEGF 164-treated mesenchyme, whereas *Flk*-1 staining was absent in the control mesenchyme after 48 h (E, F). Scale bar represents 80 mm in main panels C–F, and 200 mm in insets within C–F.

chemically defined media containing recombinant mouse VEGF 164 (100 ng/ml) appeared to be much more highly branched than the lung buds grown in control medium (Fig. 2). The stimulation of branching by VEGF was quantified by counting terminal branches (compare Figs. 2G to H). VEGF 164 increased the number of terminal branches by 60% ± 3% after 48 h (data not shown) and by 80% ± 5% after 72 h of culture ($P < 0.05$) (Fig. 2I).

Effect of VEGF 164 on Flk-1$^{nLac\text{-}Z/+}$ *expression and specific gene expression*

In order to confirm the biological activity of recombinant VEGF 164 on endothelial cells, we cultured embryonic heterozygous *Flk-1*$^{nLac\text{-}Z/+}$ lungs in the same conditions as

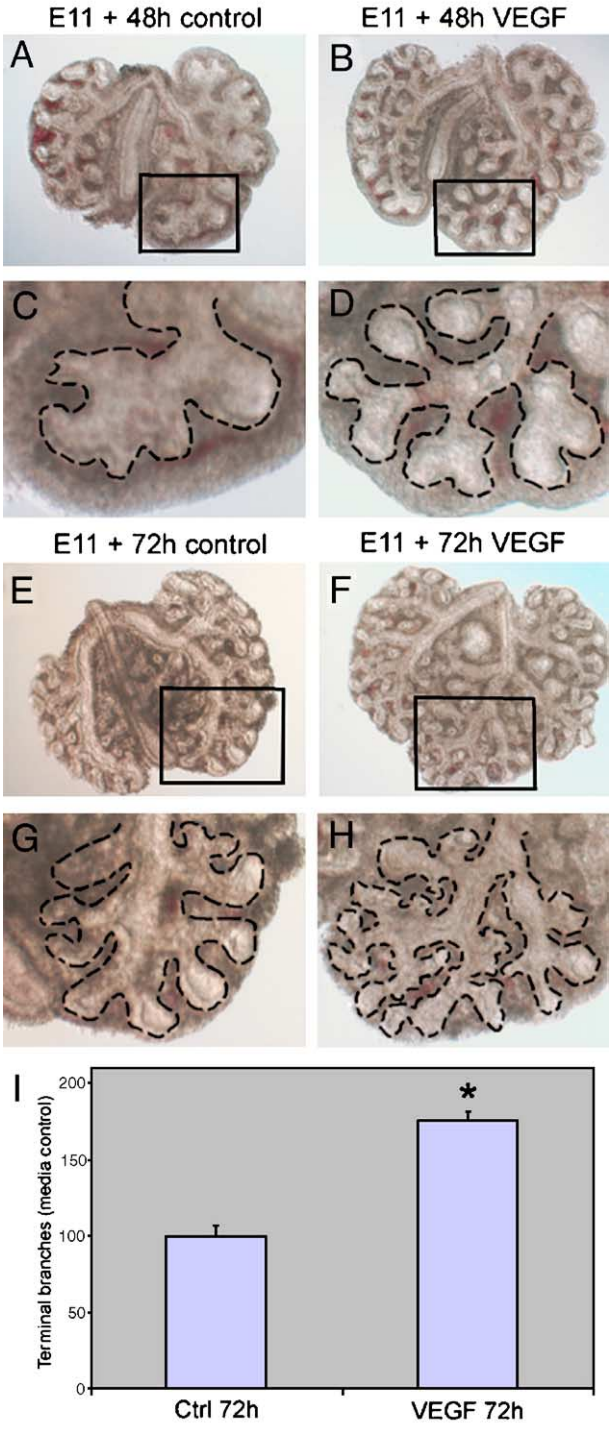

Fig. 2. VEGF 164 stimulates epithelial branching morphogenesis. E11 lungs treated with VEGF 164 (150 ng/ml) for 48 h (B) or 72 h (F) showed significantly increased epithelial branching morphogenesis compared with untreated lungs (A, E). Higher magnification of respective lungs with epithelial boundaries outlined for the purpose of illustration also showed increased branching of the endoderm in the VEGF 164-treated explants (C, D, G, H). Terminal branches were counted and VEGF 164 was found to significantly increase lung branching (*$P < 0.05$) by 60% ± 3% after 48 h (not shown) and 80% ± 5% after 72 h (I). Results are presented as means ± SD, $n = 15$, of at least 3 independent experiments.

described above for wild type lungs. A striking increase in the pattern of β-galactosidase staining and therefore in *Flk-1* expression is seen in the VEGF-treated lungs compared to the control lungs (Figs. 3A–D). Given the significant increase in branching morphogenesis, we investigated the expression of specific genes that are characteristic of FGF10 signaling pathway (*murine Sprouty2, murine Sprouty4*), bone morphogenetic protein (*Bmp-4*), as well as the specific peripheral epithelial cell marker (*Sp-c*). Increased expression of the *Sp-c* gene correlates with increasing functional maturity of the lung (Weaver, 1991). *Sp-c* is also a specific marker for the alveolar type II cell lineage. We used a sensitive competitive RT-PCR assay to measure the relative expression levels of these specific mRNAs in control versus VEGF 164-treated lungs. As expected from our previous experiments (Figs. 3A–D), we found that, compared to control lungs, exposure to exogenous VEGF 164 significantly ($P < 0.05$) increased the levels of mRNA encoding *Flk-1* receptor (142%) (Fig. 3F and Table 1). *Sp-c* expression was also increased (141%) as well as *Bmp-4* mRNA levels (139%) (Figs. 3H, J), whereas *Shh* and *Fgf10* expression remained unchanged (data not shown). In contrast, VEGF treatment decreased both *mSpry-2* and *mSpry-4* gene expression to 41% and 43% of the level of expression observed in control lungs (Figs. 3G, I).

Flk-1 antisense ODN decreases Flk-1$^{nLac-Z/+}$ expression and inhibits epithelial branching morphogenesis

Flk-1 was tested for its functional role during embryonic lung organogenesis using an antisense oligodeoxynucleotide approach. This approach also allowed us to test the functionality of *Flk-1* antisense ODN by culturing embryonic *Flk-1$^{nLac-Z/+}$* lungs in absence or presence of this oligodeoxynucleotide. As negative control and to test whether exogenous DNA sequence would be toxic to the lung explants, we also cultured *Flk-1$^{nLac-Z/+}$* lungs in a media containing a scrambled sequence comprising the same nucleotides as in the *Flk-1* antisense ODN, but in a nonsensical order termed scrambled ODN. A readily apparent decrease in β-galactosidase staining and therefore in *Flk-1* expression is seen in the *Flk-1* antisense ODN-treated lungs compared to the control versus scrambled treated lungs (Figs. 4A, C, E). The efficacy of *Flk-1* antisense ODN was confirmed by competitive PCR quantification of *Flk-1* mRNA level in cultured embryonic lungs. As shown in Fig. 5B, 40 μM *Flk-1* antisense ODN efficiently ($P < 0.05$) attenuated *Flk-1* mRNA expression by over 90% in comparison to both media control and scrambled ODN. The scrambled ODN had no inhibitory effect on *Flk-1* mRNA expression. Therefore, the observed effect upon lung branching morphogenesis with *Flk-1* antisense ODN treatment resulted from abrogation of *Flk-1* gene expression. While both control and scrambled ODN did not change lung branching (Figs. 4G, K), *Flk-1* antisense ODN caused a significant decrease of embryonic lung epithelial

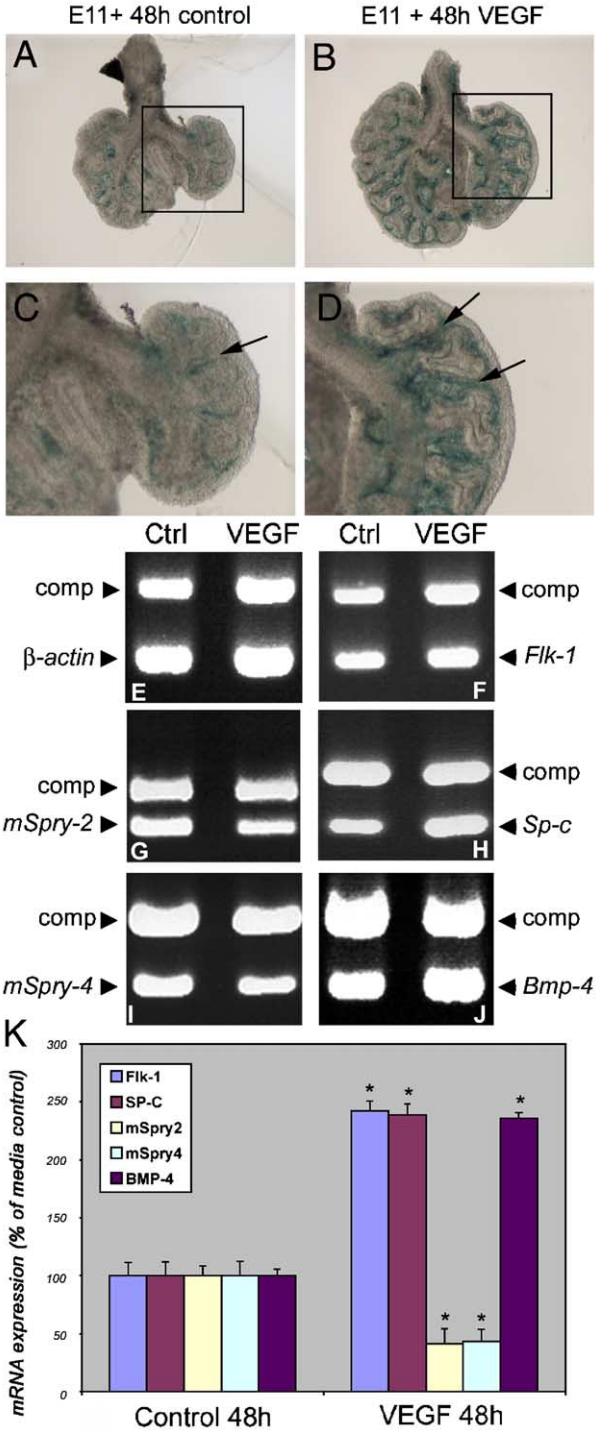

Fig. 3. VEGF 164 stimulates Flk-1 $^{n\ Lac-Z/+}$ expression. β-galactosidase staining on untreated *Flk-1$^{n\ Lac-Z/+}$* lungs (A) clearly was much less intense than in VEGF 164-treated lungs (150 ng/ml) (B). Higher magnification shows also the pattern of endothelial branching in the VEGF 164-treated lungs compared to the untreated lungs (arrows in C, D). Effect of VEGF 164 on specific gene expression (E–K). Quantification of competitive RT-PCR data by densitometric analysis with normalization to β-actin (K). VEGF 164 treatment (150 ng/ml) significantly decreased endogenous *mSpry-2* (G), *mSpry-4* (I) mRNA levels to 41% and 43% ($P < 0.05$), respectively of their level of expression observed in control lungs. While, *Flk-1* (O), *Sp-c* (Q), and *Bmp-4* (S) mRNA levels increased by 142%, 141% and 139%, respectively, in the VEGF-treated lungs compared to control lungs (*$P < 0.05$). No change in *Shh* or *Fgf10* expression was observed (not shown). Values are expressed as the mean ± SD with the medium control set at 100%. Results are presented as means ± SD, $n = 15$, combining at least 3 independent experiments.

Table 1
Quantification of competitive RT-PCR data in VEGF 164-treated vs. control lungs by densitometric measurement

Gene	Control or VEGF	Competitor or gene	Density (intensity/mm^2)	Gene/Competitor ratio	VEGF ratio/ Control ratio	Difference (%)
β-actin	Control	Competitor	2278 ± 158	1.50	1.06	+6
		Gene	3410 ± 182			
	VEGF	Competitor	2516 ± 101	1.58		
		Gene	3976 ± 226			
Flk-1	Control	Competitor	1466 ± 120	1.39	2.42	+142
		Gene	2034 ± 192			
	VEGF	Competitor	1885 ± 139	3.36		
		Gene	6334 ± 471			
Sp-c	Control	Competitor	3245 ± 324	0.63	2.41	+141
		Gene	2054 ± 251			
	VEGF	Competitor	3402 ± 274	1.53		
		Gene	5197 ± 526			
mSpy2	Control	Competitor	2857 ± 178	1.17	0.41	−59
		Gene	3334 ± 301			
	VEGF	Competitor	3039 ± 292	0.48		
		Gene	1467 ± 175			
mSpry4	Control	Competitor	4365 ± 470	0.75	0.43	−57
		Gene	3291 ± 269			
	VEGF	Competitor	4123 ± 371	0.32		
		Gene	1328 ± 184			
Bmp-4	Control	Competitor	5678 ± 283	0.57	2.39	+139
		Gene	3239 ± 196			
	VEGF	Competitor	4181 ± 125	1.37		
		Gene	5709 ± 348			

Quantification of competitive RT-PCR data by densitometric analysis. For each gene, the density of the band corresponding to the gene or the competitor was measured as Intensity/mm^2 ± SD. A ratio of gene/competitor was then determined for the control or the VEGF-treated explants. The VEGF ratio was then compared to the control ratio to determine the difference in mRNA expression in VEGF-treated versus control lung.

branching morphogenesis (Fig. 4I). As determined by the number of terminal branches, *Flk-1* antisense ODN decreased epithelial branching by 38% ± 4% at 40 μM ($P < 0.05$), while cultured explants branched normally in the presence of control media as well as in the presence of scrambled ODN (Fig. 4M).

Effect of the abrogation of Flk-1 receptor mRNA expression on specific gene expression

We evaluated specific changes in gene expression induced by the *Flk-1* antisense ODN on the cultured embryonic lungs by competitive RT-PCR (Fig. 5 and Table 2). Respectively, *mSpry2* and *mSpry4* mRNA levels increased by 162% and 142% ($P < 0.05$) in the *Flk-1* antisense ODN cultured lungs (Figs. 5C, E). In contrast, the *Sp-c* mRNA level was decreased by 59% of its expression in the control and scrambled ODN-treated lungs. Likewise, *Bmp-4* mRNA levels were also reduced by 34% in the embryonic lungs cultured with the *Flk-1* antisense ODN.

Bmp-4$^{LacZ/+}$ cultured lungs and Western analysis confirmed the respective up-regulation and downregulation of BMP-4 with VEGF 164 versus Flk-1 antisense ODN

As shown in Fig. 6, *Bmp-4$^{LacZ/+}$* cultured lungs treated with VEGF 164 clearly showed increased levels of β-galactosidase staining compared to lung cultured in control media (Figs. 6A, B). However, in presence of *Flk-1* antisense ODN, there was a significant decrease in β-galactosidase staining compared to control media and scrambled ODN-treated lungs (Figs. 6C–E). These changes in β-galactosidase staining only occurred within the distal tips of the epithelium. No changes in spatial distribution, and therefore in mesenchymal staining was observed.

The BMP-4 antibody that we used to perform Western analysis detects not only two distinct BMP-4 bands with different sizes (25 kDa, 18 kDa) corresponding to different glycosylation states of activated BMP-4, but also pro-BMP-4 (50 kDa). *Flk-1* antisense ODN reduced both pro-BMP-4 protein amount as well as the level of both glycosylated forms of activated BMP-4 (Fig. 6F). Densitometric analysis confirmed that exogenous VEGF 164 increased BMP-4 protein levels by 72% ± 6% ($P < 0.05$) compared to the lungs cultured with control media. Conversely, BMP-4 protein amount was decreased by 63% ± 7% ($P < 0.05$) in the lungs cultured with *Flk-1* antisense ODN, while the scrambled ODN at the same concentration did not have any inhibitory effect on BMP-4 proteins level. Therefore, only the *Flk-1* antisense ODN, not the scrambled ODN, resulted in a significant reduction (63%) in the BMP-4 protein level. This result was observed consistently over 3 different sets of experiments.

Effect of exogenous VEGF 164 versus Flk-1 antisense ODN on epithelial and mesenchymal cell proliferation

The respective increase or decrease in branching morphogenesis observed in lungs cultured with exogenous VEGF 164 versus *Flk-1* antisense ODN suggested that these conditions may have differentially affected the rate of

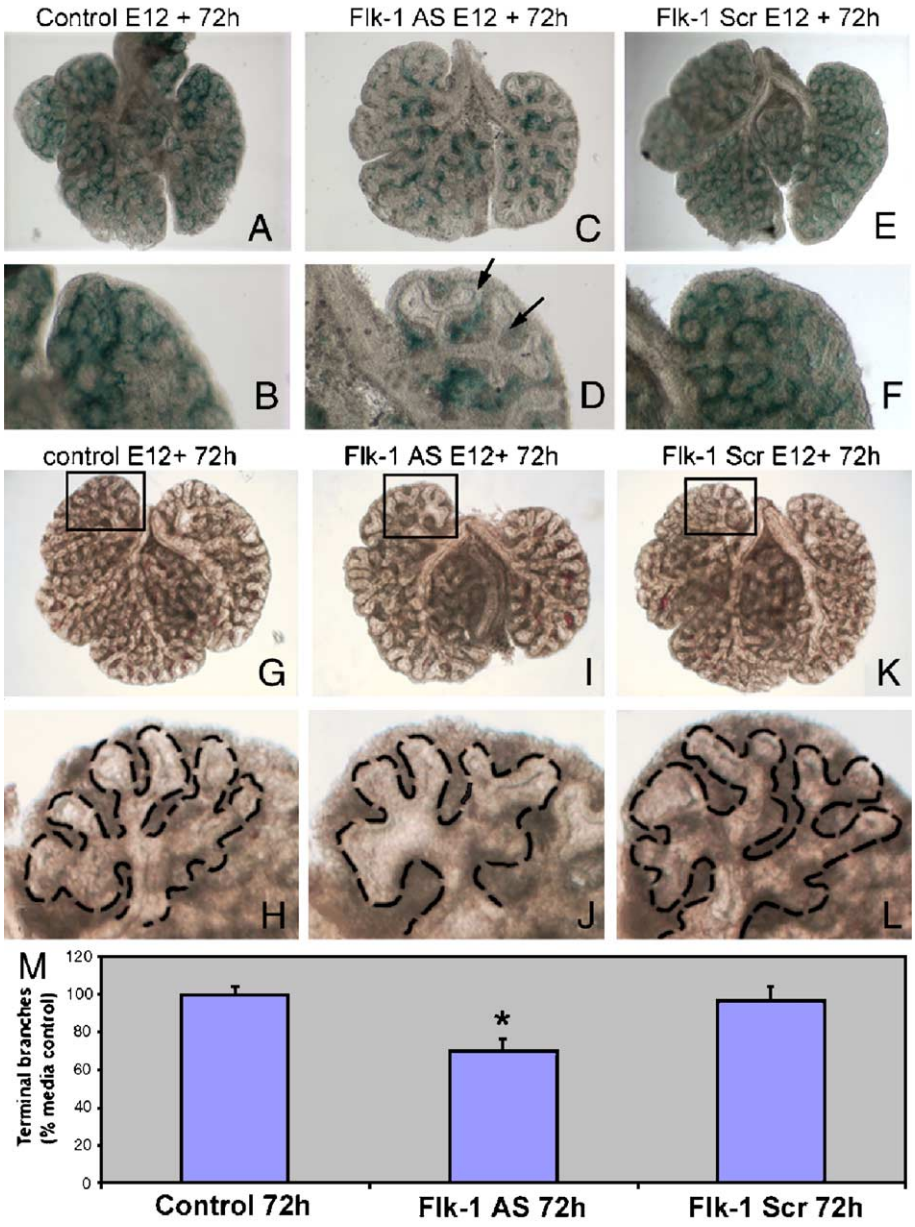

Fig. 4. *Flk-1* antisense ODN decreases *Flk-1*$^{n\ Lac\text{-}Z/+}$ expression. β-galactosidase staining in 40 μM *Flk-1* antisense ODN-treated *Flk-1*$^{n\ Lac\text{-}Z/+}$ lungs (C) was clearly decreased compared to 40 μM scrambled ODN and media control lungs (A, E). At higher magnification, endothelial branching was also clearly decreased (arrows) in the *Flk-1* antisense ODN-treated lungs (D) compared to the control and scrambled ODN-treated lungs (B, F). Abrogation of *Flk-1* (*VEGF-R2*) receptor gene expression by antisense ODN inhibits epithelial-branching morphogenesis. Lungs cultured in 40 μM *Flk-1* antisense ODN exhibit a significantly lower epithelial branching morphogenesis (I) compared with 40 μM scrambled ODN- and control-treated lungs (G, K). Higher magnification of respective lungs with outlined epithelial boundaries (H, J, L) also showed a decreased branching of the endoderm in the *Flk-1* antisense ODN-treated explants (J). After 72 h, *Flk-1* antisense ODN treatment decreased the number of terminal branches by 38% ± 4% (*$P < 0.05$) (M). Results are presented as means ± SD, $n = 15$, of at least 3 independent experiments.

cell proliferation. We therefore investigated cell proliferation by PCNA immunostaining of the lungs cultured in the different chemically defined media. The PCNA index of cells containing PCNA protein was determined as the PCNA Index. Results indicated 88% ± 3% ($P < 0.05$) more cell proliferation in the epithelium of the VEGF 164-treated explants than in controls (Fig. 7). The rate of cell proliferation in the mesenchyme increased from 21% ± 6% to 39% ± 4% ($P < 0.05$) in VEGF 164-treated explants. Conversely, the PCNA index (both epithelium and mesenchyme) was reduced from 39% ± 2% to 16% ± 2% ($P < 0.05$) in lung cultures containing *Flk-1* antisense ODN compared to control or scrambled ODN-treated lungs.

Discussion

Early embryonic lung development depends on a delicate balance between different growth factors. While endodermal

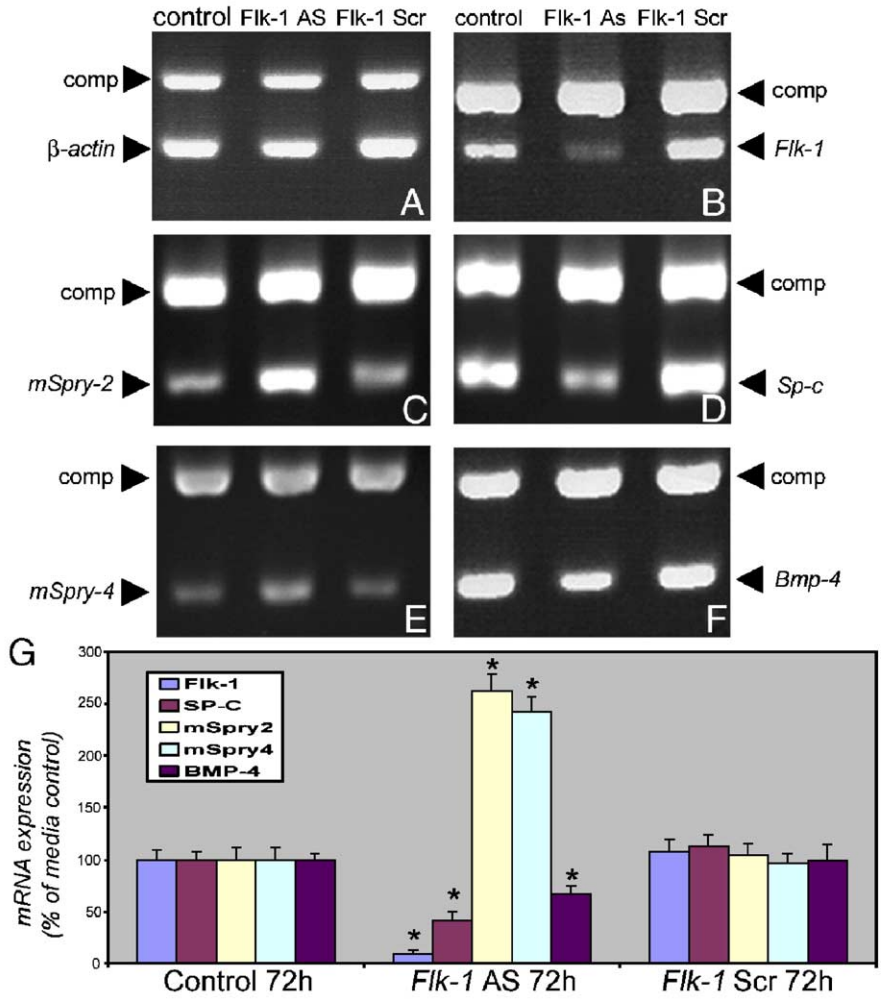

Fig. 5. Effect of the abrogation of *Flk-1* receptor mRNA expression on specific gene expression. Competitive RT-PCR data were quantified by densitometric analysis, with normalization to β-actin (G). 40 μM *Flk-1* antisense ODN significantly decreased endogenous *Flk-1* (B), *Sp-c* (D), and *Bmp-4* (F) mRNA levels by 92%, 59%, and 34% of their level of expression observed in control lungs, respectively (all $*P < 0.05$). Also 40 μM *Flk-1* antisense ODN treatment resulted in *mSpry-2* (P), *mSpry-4* (R) mRNA levels, 162% and 142% higher than those of the scrambled ODN and control medium ($*P < 0.05$). No change in *Shh* and *Fgf10* expression was observed (not shown). Values are expressed as the mean ± SD with the medium control set at 100%. Results are presented as means ± SD, $n = 15$, combining from at least 3 independent experiments.

outgrowth has been extensively studied (Hogan and Kolodziej, 2002; Warburton et al., 2000), relatively little is known about the specific role of the mesenchyme and especially endothelial cells during lung epithelial morphogenesis (Lammert et al., 2003). We therefore decided to compare the effect of exogenous VEGF 164, a specific isoform of VEGF-A, versus *Flk-1* downregulation on early mouse lung embryonic morphogenesis in our well-characterized serumless culture system. Our results demonstrate a novel positive impact of the VEGF-A signaling pathway in triggering an increase in epithelial morphogenesis. Our results also show that *Vegf-A,* expressed by the epithelium acts in a paracrine fashion on endothelial cells (Clauss et al., 1996; Keyt et al., 1996) to control epithelial morphogenesis.

In agreement with our observations, defective pulmonary development is observed in the absence of heparin sulfate-bound VEGF isoforms 164 and 188 (Galambos et al., 2002).

Interestingly, lower levels of both *Vegf-A* and *Flk-1* mRNA were found in lungs of mice overexpressing TGF-beta in the distal lung epithelium associated with an arrest in lung morphogenesis in the pseudoglandular stage (Zeng et al., 2001). Abnormal lung structure was previously associated with inhibition of the tyrosine kinase activity of Flk-1 by Su-5416 (Jakkula et al., 2000; Le Cras et al., 2002). Lower expression levels of both VEGF-A and Flk-1 were also observed in embryonic hypoplastic lungs after nitrofen treatment (Chinoy et al., 2002). In contrast, intrauterine injection of hVEGF 165 into the amniotic cavity had a pneumotrophic effect stimulating surfactant production in mice (Compernolle et al., 2002).

The herein observed enhancement of lung epithelial branching by VEGF 164 is not likely to be mediated by a direct effect of VEGF 164 on the epithelium, since *Flk-1* is expressed by the mesenchyme. Therefore, there must be a mesenchymal to epithelial relay mechanism for VEGF 164 to

Table 2
Quantification of competitive RT-PCR data in *Flk-1* antisense ODN-treated vs. control lungs or scrambled ODN-treated vs. control lungs by densitometric measurement

Gene	Control, antisense or scrambled ODN	Competitor or gene	Density (intensity/mm^2)	Gene/Competitor ratio	*Flk-1* AS ratio/Control ratio or Scrambled ratio/Control ratio	Difference (%)
β-actin	Control	Competitor	2209 ± 155	1.08	1.07	+7
		Gene	2378 ± 214			
	Flk-1 AS ODN	Competitor	1867 ± 112	1.15		
		Gene	2154 ± 108		1.02	+2
	Scrambled ODN	Competitor	2456 ± 239	1.10		
		Gene	2686 ± 192			
Flk-1	Control	Competitor	4034 ± 270	0.69	0.08	−92
		Gene	2789 ± 252			
	Flk-1 AS ODN	Competitor	4699 ± 188	0.05		
		Gene	252 ± 30		1.06	+6
	Scrambled ODN	Competitor	4526 ± 362	0.74		
		Gene	3344 ± 386			
Sp-c	Control	Competitor	4702 ± 376	0.89	0.41	−59
		Gene	4195 ± 503			
	Flk-1 AS ODN	Competitor	4999 ± 465	0.36		
		Gene	1807 ± 289		1.10	+10
	Scrambled ODN	Competitor	5056 ± 391	0.98		
		Gene	4972 ± 568			
mSpy2	Control	Competitor	4771 ± 190	0.36	2.62	+162
		Gene	1718 ± 198			
	Flk-1 AS ODN	Competitor	4814 ± 239	0.94		
		Gene	4539 ± 621		1.05	+5
	Scrambled ODN	Competitor	5050 ± 358	0.38		
		Gene	1912 ± 204			
mSpry4	Control	Competitor	3807 ± 267	0.37	2.42	+142
		Gene	1395 ± 70			
	Flk-1 AS ODN	Competitor	3614 ± 326	0.88		
		Gene	3201 ± 290		0.95	−5
	Scrambled ODN	Competitor	3586 ± 435	0.34		
		Gene	1248 ± 187			
Bmp-4	Control	Competitor	4478 ± 438	0.78	0.66	−34
		Gene	3501 ± 475			
	Flk-1 AS ODN	Competitor	4534 ± 182	0.52		
		Gene	2346 ± 194		0.98	−2
	Scrambled ODN	Competitor	4592 ± 604	0.77		
		Gene	3532 ± 539			

Quantification of competitive RT-PCR data by densitometric analysis. For each gene, the density of the band corresponding to the gene or the competitor was measured as Intensity/mm^2 ± SD. A ratio gene/competitor was determined for the control, the *Flk-1* antisense ODN, or the scrambled ODN-treated explants. The *Flk-1* antisense ratio by the control ratio was calculated to determine the difference in mRNA expression in *Flk-1* antisense-treated versus control lung. The scrambled antisense ratio by the control ratio was calculated to determine the difference in mRNA expression in scrambled antisense-treated versus control lung.

stimulate epithelial branching. This could be induced by other morphogens released by the endothelium as a result of VEGF 164 activity on these cells.

In the lung, endothelial derived signals have been shown previously to be crucial to epithelial maturation and morphogenesis. Inhibition of neovascularization by endothelial monocyte activating peptide (EMAP) II prevented endothelial cell proliferation and resulted in a marked alteration in lung morphogenesis (Schwarz et al., 2000).

In the liver, where morphogenetic signals have also been shown to come from endothelial cells, it has been observed that hepatocytes from *Flk-1* mutant embryos fail to migrate away from the epithelium. In fact, embryonic livers from *Flk-1* null mice in culture develop the initial epithelial layer but subsequently epithelial cells fail to migrate into the surrounding septum transversum (Matsumoto et al., 2001). Partial inhibition of VEGF-A in the liver also resulted in impaired organogenesis (Gerber et al., 1999).

Interestingly, endothelial signals have been shown to induce pancreatic development (Lammert et al., 2003). Remarkably, blood vessel endothelium induced insulin expression by isolated pancreatic endoderm in vitro, while removal of the dorsal aorta in *Xenopus* embryos resulted in the failure of insulin expression. Moreover, ectopic vascularization in the posterior foregut has been shown to induce ectopic insulin production (Lammert et al., 2001). The nature of the endothelial-derived signals inducing endocrine development in the pancreas is not known so far.

Since the mitogenic and differentiating effects of VEGF-164 are likely to be mainly mediated through interaction with Flk-1 receptor (Clauss et al., 1996), we investigated the expression of Flk-1 receptor using *Flk-1*$^{n\ LacZ/+}$ E14.5 lungs. At this stage of

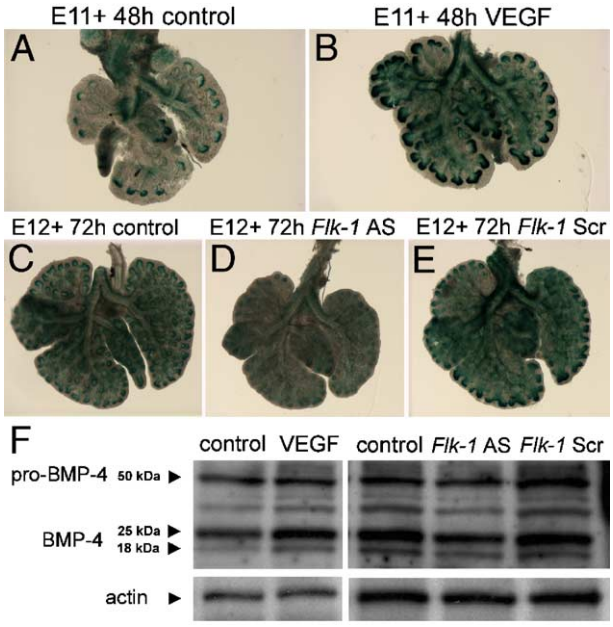

Fig. 6. Effect of exogenous VEGF 164 and of the abrogation of *Flk-1* receptor mRNA expression on *Bmp-4*$^{LacZ/+}$ expression. β-galactosidase staining in *Bmp-4*$^{LacZ/+}$ cultured lungs with exogenous VEGF 164 (B) was clearly increased compared to control lungs (A). However, in presence of *Flk-1* antisense ODN (D), there was a significant decrease in β-galactosidase staining compared to control media and scrambled ODN-treated lungs (C, E). Note that the changes in expression only occurred within the distal tips of the epithelium. Western analysis confirmed the respective up-regulation versus downregulation of BMP-4 with VEGF 164 versus *Flk-1* antisense ODN (F). Representative Western blot showing that VEGF 164 treatment (150 ng/ml) on embryonic lungs resulted in significant increased levels of BMP-4 (72% ± 6%, $P < 0.01$). Also, 40 μM *Flk-1* antisense ODN reduced BMP-4 protein expression (63% ± 7%, $P < 0.01$). Actin was used as loading control. Results are presented combining from at least 3 independent experiments.

development, we found this receptor exclusively expressed in the mesenchyme. Previous data on *Vegf-A* and *Flk-1* expression (Miquerol et al., 1999), isolated type II epithelial cells (Raoul et al., 2004), and our results on isolated endoderm show that VEGF-A does not have a proliferative or morphogenetic effect on isolated endoderm. The possible mechanism of action of VEGF-A must therefore be indirect in its role to regulate epithelial branching. VEGF 164 stimulation of intact lung explants is also associated to increased total cell proliferation as indicated by PCNA index. VEGF-A may act through Flk-1-positive cells in the mesenchyme to induce the expression of other morphogens within the mesenchyme.

Bmp-4 expression was increased following exposure to VEGF 164 in intact lung explants. However, the induction of *Bmp-4* occurred in the distal tips of the epithelium. Exogenous BMP-4 increases peripheral lung epithelial branching morphogenesis, whereas adenoviral overexpression of the BMP antagonist *gremlin* blocked the stimulatory effects of exogenous BMP-4, demonstrating that BMP-4 plays an important morphogenetic role during lung embryogenesis (Shi et al., 2001). BMP-4 is also involved in branching morphogenesis of the lung by modulating FGF10 induced morphogenesis (Weaver et al., 2000).

Interestingly, the liver phenotype of null *Flk-1* embryos is similar to *Bmp-4* deficient embryos where BMP-4 has been shown to be critical for endodermal growth (Matsumoto et al., 2001; Rossi et al., 2001). Therefore, BMP-4 may play a similar morphogenetic role during both liver and lung embryonic development.

Additionally, the expression of mouse Sprouty2 and 4, another important class of inducible regulatory molecules that have been, respectively, shown to participate in

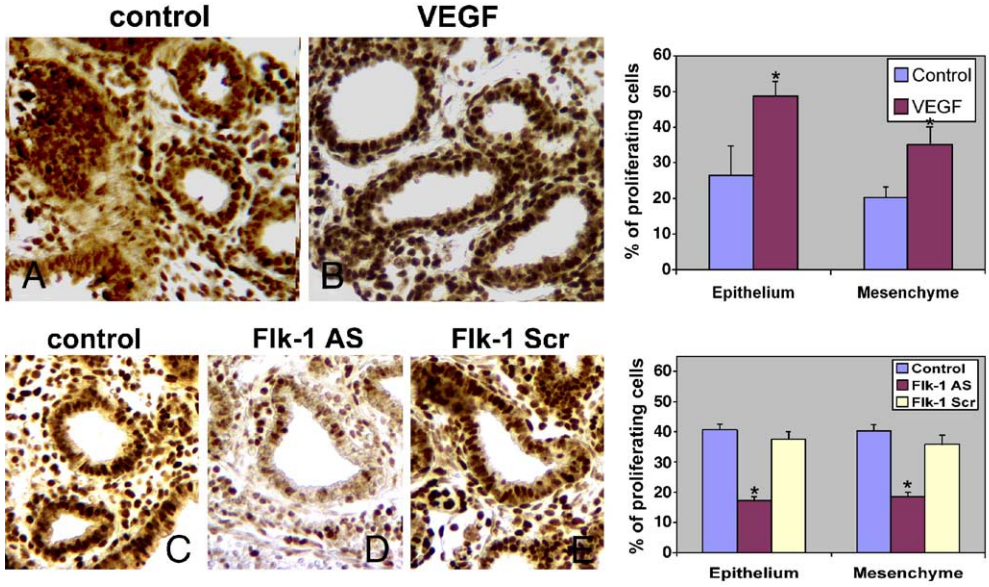

Fig. 7. Effect of exogenous VEGF 164 versus *Flk-1* antisense ODN on epithelial and mesenchymal cell proliferation. Cell proliferation analysis by PCNA immunostaining of lungs cultured in presence or absence of VEGF 164 (A, B), or in presence or absence of *Flk-1* antisense ODN (C–E). The PCNA index was increased by 88% ± 3% indicating more cell proliferation in the epithelium of the VEGF-treated explants than in the control (A, B). The rate of cell proliferation in the mesenchyme increased from 21% ± 6% to 39% ± 4% in VEGF 164-treated explants compared to control media (A, B). Conversely, *Flk-1* antisense ODN treatment decreased both epithelial and mesenchymal PCNA Index to 16% ± 2% (D) compared to 39% ± 2% in both control media and scrambled ODN-treated lungs (A, E). There were no significant differences in PCNA Index between the scrambled ODN cultured explants and the control lungs.

epithelial and endothelial morphogenesis, varies inversely to *Bmp-4* upon addition of exogenous VEGF 164 versus *Flk-1* antisense ODN. However, the respective changes in *mSpy2* and *mSpy4* expression observed are not apparently related directly to *Fgf10*, since *Fgf10* expression is not affected by exogenous VEGF 164 or *Flk-1* antisense ODN treatment. Decreased *mSpy2* expression may facilitate epithelium morphogenesis since ablation of *mSpy2* expression in cultured embryonic mouse lungs resulted in a significant increase in lung branching morphogenesis (Tefft et al., 1999). While, on the other hand, overexpression of *mSpy2* in endothelial cells revealed its potential to negatively regulate angiogenesis in response to FGF, VEGF, and EGF receptor signaling (Impagnatiello et al., 2001). Moreover, expression of *mSpy4* in endothelial cells using a recombinant adenovirus resulted in inhibition of branching and sprouting of the vasculature (Lee et al., 2001), a phenotype mediated through inhibition of MAPK activation in response to FGF and VEGF. *mSpy4* is also critical during the pseudoglandular stage of embryonic lung morphogenesis, since in vivo overexpression of *mSpy4* during this time period resulted in severe defects in lobulation and lung hypoplasia (Perl et al., 2003).

Herein, we show that VEGF-A signaling acts as a morphogen, inducing a significant increase in both epithelial and endothelial branching morphogenesis in the early embryonic mouse lung in culture. However, the stimulating effect of VEGF-A on the epithelium is probably indirect since *Flk-1* is only expressed in the mesenchyme. We also demonstrated that epithelial *Bmp-4* expression is, respectively, increased by stimulation versus decreased by inhibition of the VEGF-A signaling pathway, while the other changes in *mSpy2 and 4* expression are the inverse of *Bmp-4*. Thus, VEGF-A signaling exerts a positive role on lung epithelial and endothelial morphogenesis. We speculate that VEGF-A signals function in a critical morphogenetic role by mediating epithelial–endothelial/mesenchymal cross talk.

Acknowledgments

We thank Pablo Bringas and Valentino Santos for their technical expertise. This work was supported in part by HL75773 (DW), HL 44977 (DW), HL 44060 (DW), HL 60231 (DW), HL 074832-01 (SB), American Lung Association (SB) and also in part by the Saban Research Institute Predoctoral award to Pierre-Marie Del Moral.

References

Acosta, J.M., Thebaud, B., Castillo, C., Mailleux, A., Tefft, D., Wuenschell, C., Anderson, K.D., Bourbon, J., Thiery, J.P., Bellusci, S., Warburton, D., 2001. Novel mechanisms in murine nitrofen-induced pulmonary hypoplasia: FGF-10 rescue in culture. Am. J. Physiol.: Lung Cell. Mol. Physiol. 281, L250–L257.

Barleon, B., Sozzani, S., Zhou, D., Weich, H.A., Mantovani, A., Marme, D., 1996. Migration of human monocytes in response to vascular endothelial growth factor (VEGF) is mediated via the VEGF receptor flt-1. Blood 87, 3336–3343.

Bellusci, S., Grindley, J., Emoto, H., Itoh, N., Hogan, B.L., 1997. Fibroblast growth factor 10 (FGF10) and branching morphogenesis in the embryonic mouse lung. Development 124, 4867–4878.

Carmeliet, P., Ferreira, V., Breier, G., Pollefeyt, S., Kieckens, L., Gertsenstein, M., Fahrig, M., Vandenhoeck, A., Harpal, K., Eberhardt, C., Declercq, C., Pawling, J., Moons, L., Collen, D., Risau, W., Nagy, A., 1996. Abnormal blood vessel development and lethality in embryos lacking a single VEGF allele. Nature 380, 435–439.

Chinoy, M.R., Graybill, M.M., Miller, S.A., Lang, C.M., Kauffman, G.L., 2002. Angiopoietin-1 and VEGF in vascular development and angiogenesis in hypoplastic lungs. Am. J. Physiol.: Lung Cell. Mol. Physiol. 283, L60–L606.

Chuang, P.T., McMahon, A.P., 2003. Branching morphogenesis of the lung: new molecular insights into an old problem. Trends Cell Biol. 13, 86–91.

Clauss, M., Weich, H., Breier, G., Knies, U., Rockl, W., Waltenberger, J., Risau, W., 1996. The vascular endothelial growth factor receptor Flt-1 mediates biological activities. Implications for a functional role of placenta growth factor in monocyte activation and chemotaxis. J. Biol. Chem. 271, 17629–17634.

Compernolle, V., Brusselmans, K., Acker, T., Hoet, P., Tjwa, M., Beck, H., Plaisance, S., Dor, Y., Keshet, E., Lupu, F., Nemery, B., Dewerchin, M., Van Veldhoven, P., Plate, K., Moons, L., Collen, D., Carmeliet, P., 2002. Loss of HIF-2alpha and inhibition of VEGF impair fetal lung maturation, whereas treatment with VEGF prevents fatal respiratory distress in premature mice. Nat. Med. 8, 702–710.

Ferrara, N., Carver-Moore, K., Chen, H., Dowd, M., Lu, L., O'Shea, K.S., Powell-Braxton, L., Hillan, K.J., Moore, M.W., 1996. Heterozygous embryonic lethality induced by targeted inactivation of the VEGF gene. Nature 380, 439–442.

Ferrara, N., Gerber, H.P., LeCouter, J., 2003. The biology of VEGF and its receptors. Nat. Med. 9, 669–676.

Fong, G.H., Rossant, J., Gertsenstein, M., Breitman, M.L., 1995. Role of the Flt-1 receptor tyrosine kinase in regulating the assembly of vascular endothelium. Nature 376, 66–70.

Galambos, C., Ng, Y.S., Ali, A., Noguchi, A., Lovejoy, S., D'Amore, P.A., DeMello, D.E., 2002. Defective pulmonary development in the absence of heparin-binding vascular endothelial growth factor isoforms. Am. J. Respir. Cell Mol. Biol. 27, 194–203.

Gebb, S.A., Shannon, J.M., 2000. Tissue interactions mediate early events in pulmonary vasculogenesis. Dev. Dyn. 217, 159–169.

Gerber, H.P., Hillan, K.J., Ryan, A.M., Kowalski, J., Keller, G.A., Rangell, L., Wright, B.D., Radtke, F., Aguet, M., Ferrara, N., 1999. VEGF is required for growth and survival in neonatal mice. Development 126, 1149–1159.

Greenberg, J.M., Thompson, F.Y., Brooks, S.K., Shannon, J.M., McCormick-Shannon, K., Cameron, J.E., Mallory, B.P., Akeson, A.L., 2002. Mesenchymal expression of vascular endothelial growth factors D and A defines vascular patterning in developing lung. Dev. Dyn. 224, 144–153.

Healy, A.M., Morgenthau, L., Zhu, X., Farber, H.W., Cardoso, W.V., 2000. VEGF is deposited in the subepithelial matrix at the leading edge of branching airways and stimulates neovascularization in the murine embryonic lung. Dev. Dyn. 219, 341–352.

Hiratsuka, S., Minowa, O., Kuno, J., Noda, T., Shibuya, M., 1998. Flt-1 lacking the tyrosine kinase domain is sufficient for normal development and angiogenesis in mice. Proc. Natl. Acad. Sci. U. S. A. 95, 9349–9354.

Hogan, B.L., Kolodziej, P.A., 2002. Organogenesis: molecular mechanisms of tubulogenesis. Nat. Rev., Genet. 3, 513–523.

Hogan, B.L., Yingling, J.M., 1998. Epithelial/mesenchymal interactions and branching morphogenesis of the lung. Curr. Opin. Genet. Dev. 8, 481–486.

Impagnatiello, M.A., Weitzer, S., Gannon, G., Compagni, A., Cotten, M., Christofori, G., 2001. Mammalian sprouty-1 and-2 are membrane-anchored phosphoprotein inhibitors of growth factor signaling in endothelial cells. J. Cell Biol. 152, 1087–1098.

Jaskoll, T.F., Don-Wheeler, G., Johnson, R., Slavkin, H.C., 1988. Embryonic mouse lung morphogenesis and type II cytodifferentiation in serumless, chemically defined medium using prolonged in vitro cultures. Cell Differ. 24, 105–117.

Jakkula, M., Le Cras, T.D., Gebb, S., Hirth, K.P., Tuder, R.M., Voelkel, N.F., Abman, S.H., 2000. Inhibition of angiogenesis decreases alveolarization in

the developing rat lung. Am. J. Physiol.: Lung Cell. Mol. Physiol. 279, L600–L607.
Keyt, B.A., Berleau, L.T., Nguyen, H.V., Chen, H., Heinsohn, H., Vandlen, R., Ferrara, N., 1996. The carboxyl-terminal domain (111–165) of vascular endothelial growth factor is critical for its mitogenic potency. J. Biol. Chem. 271, 7788–7795.
Lammert, E., Cleaver, O., Melton, D., 2001. Induction of pancreatic differentiation by signals from blood vessels. Science 294, 564–567.
Lammert, E., Cleaver, O., Melton, D., 2003. Role of endothelial cells in early pancreas and liver development. Mech. Dev. 120, 59–64.
Lawson, K.A., Dunn, N.R., Roelen, B.A., Zeinstra, L.M., Davis, A.M., Wright, C.V., Korving, J.P., Hogan, B.L., 1999. Bmp4 is required for the generation of primordial germ cells in the mouse embryo. Genes Dev. 13, 424–436.
Le Cras, T.D., Markham, N.E., Tuder, R.M., Voelkel, N.F., Abman, S.H., 2002. Treatment of newborn rats with a VEGF receptor inhibitor causes pulmonary hypertension and abnormal lung structure. Am. J. Physiol.: Lung Cell. Mol. Physiol. 283, L555–L562.
Lee, S.H., Schloss, D.J., Jarvis, L., Krasnow, M.A., Swain, J.L., 2001. Inhibition of angiogenesis by a mouse sprouty protein. J. Biol. Chem. 276, 4128–4133.
Leung, D.W., Cachianes, G., Kuang, W.J., Goeddel, D.V., Ferrara, N., 1989. Vascular endothelial growth factor is a secreted angiogenic mitogen. Science 246, 1306–1309.
Marchand, G.S., Noiseux, N., Tanguay, J.F., Sirois, M.G., 2002. Blockade of in vivo VEGF-mediated angiogenesis by antisense gene therapy: role of Flk-1 and Flt-1 receptors. Am. J. Physiol.: Heart Circ. Physiol. 282, H194–H204.
Matsumoto, K., Yoshitomi, H., Rossant, J., Zaret, K.S., 2001. Liver organogenesis promoted by endothelial cells prior to vascular function. Science 294, 559–563.
Miquerol, L., Gertsenstein, M., Harpal, K., Rossant, J., Nagy, A., 1999. Multiple developmental roles of VEGF suggested by a LacZ-tagged allele. Dev. Biol. 212, 307–322.
Miquerol, L., Langille, B.L., Nagy, A., 2000. Embryonic development is disrupted by modest increases in vascular endothelial growth factor gene expression. Development 127, 3941–3946.
Ng, Y.S., Rohan, R., Sunday, M.E., Demello, D.E., D'Amore, P.A., 2001. Differential expression of VEGF isoforms in mouse during development and in the adult. Dev. Dyn. 220, 112–121.
Perl, A.K., Hokuto, I., Impagnatiello, M.A., Christofori, G., Whitsett, J.A., 2003. Temporal effects of Sprouty on lung morphogenesis. Dev. Biol. 258, 154–168.
Raoul, W., Chailley-Heu, B., Barlier-Mur, A.M., Delacourt, C., Maitre, B., Bourbon, J.R., 2004. Effects of vascular endothelial growth factor on isolated fetal alveolar type II cells. Am. J. Physiol.: Lung Cell. Mol. Physiol. 286, L1293–L1301.
Rossi, J.M., Dunn, N.R., Hogan, B.L., Zaret, K.S., 2001. Distinct mesodermal signals, including BMPs from the septum transversum mesenchyme, are required in combination for hepatogenesis from the endoderm. Genes Dev. 15, 1998–2009.
Schwarz, M.A., Zhang, F., Gebb, S., Starnes, V., Warburton, D., 2000. Endothelial monocyte activating polypeptide II inhibits lung neovascularization and airway epithelial morphogenesis. Mech. Dev. 95, 123–132.
Shalaby, F., Rossant, J., Yamaguchi, T.P., Gertsenstein, M., Wu, X.F., Breitman, M.L., Schuh, A.C., 1995. Failure of blood-island formation and vasculogenesis in Flk-1-deficient mice. Nature 376, 62–66.
Shi, W., Zhao, J., Anderson, K.D., Warburton, D., 2001. Gremlin negatively modulates BMP-4 induction of embryonic mouse lung branching morphogenesis. Am. J. Physiol.: Lung Cell. Mol. Physiol. 280, L1030–L1039.
Shima, D.T., Kuroki, M., Deutsch, U., Ng, Y.S., Adamis, A.P., D'Amore, P.A., 1996. The mouse gene for vascular endothelial growth factor. Genomic structure, definition of the transcriptional unit, and characterization of transcriptional and post-transcriptional regulatory sequences. J. Biol. Chem. 271, 3877–3883.
Tefft, J.D., Lee, M., Smith, S., Leinwand, M., Zhao, J., Bringas Jr., P., Crowe, D.L., Warburton, D., 1999. Conserved function of mSpry-2, a murine homolog of *Drosophila* sprouty, which negatively modulates respiratory organogenesis. Curr. Biol. 9, 219–222.
Warburton, D., Seth, R., Shum, L., Horcher, P.G., Hall, F.L., Werb, Z., Slavkin, H.C., 1992. Epigenetic role of epidermal growth factor expression and signalling in embryonic mouse lung morphogenesis. Dev. Biol. 149, 123–133.
Warburton, D., Schwarz, M., Tefft, D., Flores-Delgado, G., Anderson, K.D., Cardoso, W.V., 2000. The molecular basis of lung morphogenesis. Mech. Dev. 92, 55–81.
Weaver, T.E., 1991. Surfactant proteins and SP-D. Am. J. Respir. Cell Mol. Biol. 5, 4–5.
Weaver, M., Dunn, N.R., Hogan, B.L., 2000. Bmp4 and Fgf10 play opposing roles during lung bud morphogenesis. Development 127, 2695–2704.
Yoshida, A., Anand-Apte, B., Zetter, B.R., 1996. Differential endothelial migration and proliferation to basic fibroblast growth factor and vascular endothelial growth factor. Growth Factors 13, 57–64.
Zeng, X., Gray, M., Stahlman, M.T., Whitsett, J.A., 2001. TGF-beta1 perturbs vascular development and inhibits epithelial differentiation in fetal lung in vivo. Dev. Dyn. 221, 289–301.
Zhao, J., Lee, M., Smith, S., Warburton, D., 1998. Abrogation of Smad3 and Smad2 or of Smad4 gene expression positively regulates murine embryonic lung branching morphogenesis in culture. Dev. Biol. 194, 182–195.